Systematic study of (n,p) reaction cross sections from the reaction threshold to 20 MeV

B. Lalremruata,[1,*] N. Otuka,[2] G. J. Tambave,[3] V. K. Mulik,[4] B. J. Patil,[4] S. D. Dhole,[4] A. Saxena,[5] S. Ganesan,[6] and V. N. Bhoraskar[4]

[1]*Department of Physics, Mizoram University, Aizawl-796004, India*
[2]*Nuclear Data Section, International Atomic Energy Agency, A-1400 Wien, Austria*
[3]*Kernfysisch Versneller Instituut, Zernikelaan 25, NL-9747 AA Groningen, The Netherlands*
[4]*Department of Physics, University of Pune, Pune-411007, India*
[5]*Nuclear Physics Division, Bhabha Atomic Research Centre, Mumbai-400085, India*
[6]*Ex-Reactor Physics Design Division, Bhabha Atomic Research Centre, Mumbai-400085, India*

(Received 7 December 2011; revised manuscript received 1 February 2012; published 29 February 2012; corrected 6 April 2012)

The cross sections of ^{nat}Cr$(n,x)^{52}$V, ^{52}Cr$(n,p)^{52}$V, ^{nat}Cr$(n,x)^{53}$V, ^{53}Cr$(n,p)^{53}$V, ^{nat}Zn$(n,x)^{66}$Cu, ^{66}Zn$(n,p)^{66}$Cu, ^{nat}Zn$(n,x)^{68}$Cu^{m}, ^{68}Zn$(n,p)^{68}$Cu^{m}, ^{nat}Mo$(n,x)^{97}$Nb^{g}, ^{97}Mo$(n,p)^{97}$Nb^{g}, ^{nat}Mo$(n,x)^{97}$Nb^{m}, ^{97}Mo$(n,p)^{97}$Nb^{m}, ^{nat}Sn$(n,x)^{116}$In^{m1+m2}, ^{116}Sn$(n,p)^{116}$In^{m1+m2}, ^{nat}Sn$(n,x)^{117}$In^{g}, ^{117}Sn$(n,p)^{117}$In^{g}, ^{nat}Sn$(n,x)^{118}$In^{m1+m2}, ^{118}Sn$(n,p)^{118}$In^{m1+m2}, ^{nat}Sn$(n,x)^{120}$In^{x}, ^{120}Sn$(n,p)^{120}$In^{x}, ^{nat}Ba$(n,x)^{138}$Cs, and ^{138}Ba$(n,p)^{138}$Cs reactions have been measured at 14.8 MeV neutron energy. In the present work, the contributions of (n,np), (n,pn), and (n,d) reactions from heavier isotopes are subtracted. The cross sections were also estimated with the TALYS-1.2 nuclear model code using different level density models, at neutron energies varying from the reaction threshold to 20 MeV. The variations in the (n,p) cross sections with the neutron number in the isotopes of an element are also discussed in brief.

DOI: 10.1103/PhysRevC.85.024624 PACS number(s): 21.10.Ma, 24.60.Dr, 25.40.−h

I. INTRODUCTION

The cross sections of a number of neutron-induced (n,p) reactions are required for design calculations in nuclear reactors and other related technology. One of the problems normally faced in the development of fusion reactors is the generation of charged particles through the fast-neutron-induced reactions such as (n,p), (n,α), $(n,n'\alpha)$, and $(n,n'p)$. Such reactions are induced by bombardment of fast neutrons on the elements of the first wall, structural, and blanket components of the reactors. These nuclear reactions lead to the formation of hydrogen and helium gases in the reactor wall at different locations. In addition, other processes such as atomic displacements and transmutations, etc., can produce microstructural defects in the materials used in and around the reactor. The mechanical properties of the reactor materials may become deteriorated in the course of time, particularly when the neutron fluence becomes very high. The work related to the development of radiation-resistant materials for applications in reactors has therefore gained importance in recent years. For this purpose, as well as for other applications, accurate values of the cross sections for the production of hydrogen and helium in the reactor materials through nuclear reactions induced by neutrons of energy up to 20 MeV are required. These cross sections are also important for estimating the level of nuclear heating and other parameters such as primary knock-on atom (PKA) and displacement per atom (DPA) [1] required for radiation damage studies. This experimental paper has been motivated by the nuclear data needs of advanced nuclear energy systems. The design and development of innovative thermal, fast, fusion, fission-fusion, and accelerator driven systems all require new and improved nuclear data for a sound scientific understanding [2].

Although 14-MeV neutron-induced reactions have been extensively studied, especially by using the activation technique due to the availability of monoenergetic neutrons from D-T reactions, however, existing data show large discrepancies between the reported cross sections for a target at the same neutron energy, and it is therefore difficult to fix and optimize the statistical model parameters. The comparison with the theoretical analysis, especially for (n,p) reactions, is extremely unsatisfactory. In some of the cases, the experimental cross sections and the corresponding theoretical cross sections differ by a large magnitude. Direct, pre-equilibrium (PE) and statistical processes should be considered in order to account for reaction channels that play an important role in fast-neutron interactions for neutron energies up to 20 MeV. To assess the impact of different model assumptions and for the determination of the optimum parameters that are needed to describe these processes comprehensively, measurements that address the dominant reaction channels are essential [3]. It is therefore important to repeat measurements with better accuracy so that the new and improved measured data sets can help in understanding these reactions in terms of statistical models and in the better evaluation of these reaction cross sections in the future.

In the present paper, selected (n,p) reaction cross sections for elements important for the structural, cooling, and shielding materials in the mass region 50–140 have been experimentally measured. The choice of the reactions is made on the basis of large discrepancies in the reported cross sections or if the measured data are very few around 14.8-MeV neutron energy and for reactions with product nuclei having relatively short half-lives(less than 1 h) which are suitable for our present experimental setup. The cross sections measured in the present

*marema08@gmail.com

work have been compared with the literature values from the EXFOR database [4], the Evaluated Nuclear Data File (ENDF), and also with theoretical model calculations using the TALYS-1.2 [5] nuclear model code.

II. EXPERIMENT

A. Experimental setup

For this work, the 14-MeV neutron generator (Cockcroft-Walton) of the Department of Physics, University of Pune was used. The 14.8-MeV neutrons were produced through the ^{3}H(d,n)^{4}He reaction (Q = 17.59 MeV), in which an 8.6-Ci tritium target was bombarded by deuterium ions of energy ∼150 keV at a deuteron beam current ∼100 μA. Samples were irradiated at a 0° angle relative to the incident deuteron beam. The distance between the sample and the tritium target was ∼10 mm.

B. Samples

Almost all the reaction cross sections have been measured using powders of pure chemical compounds of the respective elements. However, for molybdenum a thin foil was used. Each sample was made by packing a known weight of the powder of the element along with pure aluminum foils of known weight in a polyethylene bag. The weight measurement of the sample was accurate to 100 μg. The elemental powder and foil were sandwiched between the aluminum monitor foils, and in this manner, three samples for each reaction were prepared and the size of each sample was ∼15 mm × 15 mm and ∼2 mm thick. Table I gives the details of the isotopes, elements, and compounds used for the sample.

C. Neutron irradiation and measurement of γ-ray activity

Each sample was irradiated with 14.8-MeV neutrons. After completion of the irradiation period, the sample was transferred to the counting room. The γ-ray activity was measured by a lead-shielded high-purity germanium (HPGe) detector having 38% relative efficiency, and 1.8-keV energy resolution at 1.33-MeV γ energy. The detector was connected to a personal-computer-based multichannel analyzer (MCA). The area under each photo peak was determined with a Canberra Genie-2k system. The photo-peak efficiency of the HPGe detector in the geometry used was determined using standard sources (^{22}Na, ^{54}Mn, ^{57}Co, ^{60}Co, ^{133}Ba, ^{137}Cs) to an uncertainty within 3%. The coincidence corrections were incorporated following the method and magnitude given in the literature [6]. The reaction ^{27}Al(n,p)^{27}Mg was used as a monitor reaction. The radioisotope ^{27}Mg has a half-life of 9.46 min and emits γ rays of energy 0.844 MeV with 71.8% intensity [7]. The standard value of the ^{27}Al(n,p)^{27}Mg reaction cross section is σ_m = 62.9 ± 1.4 mb at 14.81-MeV incident neutron energy [8]. The reaction ^{27}Al(n,α)^{24}Na was also used as the monitor reaction in the study of the ^{97}Mo(n,p)^{97}Nb^{g} reaction. The radioisotope ^{24}Na has a half-life of 14.997 h, and emits γ rays of energy 1.369 MeV with 99.99% intensity [7]. The standard value of the ^{27}Al(n,α)^{24}Na reaction cross section is σ_m = 113.3 ± 2.3 mb at 14.78-MeV incident neutron energy [9]. The neutron flux has also been monitored throughout the experiment, and the activity measured from the radioactive decay of ^{27}Mg and ^{24}Na produced by the reaction ^{27}Al(n,p)^{27}Mg and ^{27}Al(n,α)^{24}Na using the same monitoring foil has been used. The flux of the neutron has been observed to be constant within 2% and the nominal neutron flux was ∼5×10^{7} neutrons/cm^{2} s.

D. Estimation of the cross section

The natural sample cross section σ_x of a neutron-induced nuclear reaction can be estimated relative to the cross section σ_m of the monitor reaction by using the following relation [10]:

$$\sigma_x = \sigma_m \frac{A_x \varepsilon_m f_m \lambda_x}{A_m \varepsilon_x f_x \lambda_m} \frac{N_m}{N_x} \frac{(1-e^{-\lambda_m t_1})}{(1-e^{-\lambda_x t_1})} \frac{e^{-\lambda_m t_2}}{e^{-\lambda_x t_2}} \frac{(1-e^{-\lambda_m t_3})}{(1-e^{-\lambda_x t_3})}. \quad (1)$$

TABLE I. Details of the isotopes, elements and compounds used for the cross section measurement. The isotopic abundance adopted in the current cross section derivation is taken from Ref. [7].

Target material	Weight of the sample (g)	Isotope of interest	Isotopic abundance (%)
Al	0.4746	^{27}Al	100
Cr_2O_3	1.3097	^{52}Cr	83.79
		^{53}Cr	9.50
		^{54}Cr	2.36
ZnO	1.3664	^{66}Zn	27.90
		^{67}Zn	4.10
		^{68}Zn	18.75
Mo	1.3383	^{97}Mo	9.55
		^{98}Mo	24.13
Sn	4.0179	^{116}Sn	14.54
		^{117}Sn	7.68
		^{118}Sn	24.22
		^{119}Sn	8.59
		^{120}Sn	32.58
$Ba(ClO_3)_2 \cdot H_2O$	1.4707	^{138}Ba	71.69

TABLE II. Nuclear reactions, their corresponding decay data [7], and the irradiation, cooling, and counting times (in minutes).

Reaction	Half-life (min)	γ energy (MeV)	γ intensity (%)	Irradiation time (min)	Cooling time (min)	Counting time (min)
$^{nat}Cr(n,x)^{52}V$	3.743	1.434	100	3	0.33	2
$^{nat}Cr(n,x)^{53}V$	1.543	1.006	89.6	3	0.33	2
$^{nat}Zn(n,x)^{66}Cu$	5.12	1.039	9.2	5	2.33	5
$^{nat}Zn(n,x)^{68}Cu^{m}$	3.75	0.526	73.3	5	2.33	5
$^{nat}Mo(n,x)^{97}Nb^{g}$	72.10	0.657	98.2	5	0.33	5
$^{nat}Mo(n,x)^{97}Nb^{m}$	0.978	0.743	97.9	5	0.33	1.01
$^{nat}Sn(n,x)^{116}In^{m1+m2}$	54.29	0.417	27.2	5	1.28	5
		1.293	84.8			
$^{nat}Sn(n,x)^{117}In^{g}$	43.2	0.553	100	5	1.28	5
$^{nat}Sn(n,x)^{118}In^{m1+m2}$	4.45	0.683	54.3	5	1.28	5
$^{nat}Sn(n,x)^{120}In^{x}$	0.051	1.173	19.0	5	0.25	1.02
	0.788	1.171	100			
	0.770	1.171	97.5			
$^{nat}Ba(n,p)^{138}Cs$	33.41	1.436	76.3	5	0.33	5

where A is the number of counts under the photo peak, f is the photon disintegration probability, ε is the detector efficiency, σ is the reaction cross section, λ is the decay constant, N is the number of atoms of the elemental natural sample, t_1 is the irradiation time, t_2 is the cooling time, and t_3 is the period for which the gamma activity is measured. The quantities with the subscripts x and m are for the studied and monitor reactions, respectively. The details of the energies and branching ratios of the γ rays adopted in the cross-section estimation, the irradiation time, cooling time, and counting time are given in Table II.

For reactions where the heavier isotopes in the elemental sample produce the final residual product nuclei, the contributions of the (n,np), (n,pn), and (n,d) reactions to the isotopic (n,p) cross section have been taken into account. The isotopic (n,p) reaction cross section is derived by subtracting the available measured cross sections for the competing reactions. For example, the isotopic $^{52}Cr(n,p)^{52}V$ reaction cross section has been derived by subtracting the $^{53}Cr(n,x)^{52}V$ measured cross sections multiplied by ^{53}Cr isotopic abundance from the present $^{nat}Cr(n,x)^{52}V$ measured cross sections, and then dividing by the ^{52}Cr isotopic abundance. Hence,

$$\sigma[^{52}Cr(n,p)^{52}V] = \{\sigma[^{nat}Cr(n,x)^{52}V] - a(^{53}Cr)\sigma[^{53}Cr(n,x)^{52}V]\}/a(^{52}Cr), \quad (2)$$

where a stands for isotopic abundance. The same procedure has been used for heavier mass isotopes.

The general equation for the isotopic cross section similar to Eq. (2) can then be written as

$$\sigma(n,p) = \{\sigma_x - [a_h\sigma(n,x)]\}/a_i, \quad (3)$$

where σ_x is the elemental cross section given by Eq. (1), and a_h is the isotopic abundance of a heavier isotope contributing to the isotopic cross section through (n,np) and (n,d) reactions. $\sigma(n,x)$ is the heavier isotopic cross section taken from literature measured cross sections, and a_i is the isotopic abundance of the isotope of interest in the present paper.

In the case of isotopes, where no stable heavier isotopes are present and cannot contribute through (n,np), (n,d), the isotopic (n,p) cross section has been derived by

$$\sigma(n,p) = \sigma_x/a_i, \quad (4)$$

where the symbols have their usual meanings.

E. Estimation of the uncertainties

The uncertainties associated with the measured cross sections include uncertainties in (i) counting statistics 2–9%, (ii) detector efficiency ~3%, (iii) γ-ray self-absorption ~1%, (iv) coincidence summing effects ~1%, (v) neutron flux fluctuations ~2%, (vi) monitor cross sections ~2.2%, (vii) decay data ~2%, and (viii) dead time ~1.5%. Total uncertainties were estimated in quadrature by taking the square root of the sum of the squares of the individual uncertainties.

III. NUCLEAR MODELS

The excitation functions for the reactions were studied theoretically by using the nuclear model code TALYS-1.2 [5]. The optical model parameters for neutrons and protons were obtained by a local potential proposed by Koning and Delaroche [11]. Similarly, the folding approach of Watanabe [12] was used for α particles. The compound nucleus contribution was calculated by the Hauser-Feshbach model [13]. The two-component exciton model developed by Kalbach [14] was used for calculating the pre-equilibrium contribution.

The level density parameters were calculated by using five different choices of the level density model available in TALYS-1.2 [5]. The five level density models are as follows: (i) ldmodel1 is the constant temperature and Fermi-gas model,

where the constant temperature model is used in the low excitation region and the Fermi-gas model is used in the high excitation energy region. The transition energy is around the neutron separation energy. (ii) ldmodel2 is the back-shifted Fermi-gas model. (iii) ldmodel3 is the generalized superfluid model. (iv) ldmodel4 are microscopic level densities from Goriely's table [15]. (v) ldmodel5 are microscopic level densities from Hilaire's table [15]. The theoretical calculations have been done using the default parameter values, with the only change being made is the choice of the level density models.

IV. RESULTS AND DISCUSSION

To get a consistent and meaningful comparison between data measured by using the activation method, the following points are taken into account. First, when a decay γ line branching ratio was used previously that was very much different from the one used in the present paper, which is the latest decay data available [7], normalization of previously measured data is performed and cross sections are compared, and where such a normalization is done, it is reported in the text. However, differences in the half-lifes used previously are ignored while comparing the measured data between themselves. Second, for reactions in which heavier isotopes of the same element contribute to the measured (n,p) cross section, a check for each data point is done for the correction of this contribution, and are reported and discussed in the text. Third, while comparing our present result at 14.8 MeV with previously reported data at the same energy, the above two points as well as the consistency of the monitor reaction cross section is checked.

In all the plots, the data points represent the present measured cross sections at 14.8-MeV neutron energy as well as all the measured cross sections previously reported in the literature, which are available in the EXFOR database [4]. The previously measured cross sections reported in the literature are divided into four groups: (1) measurements carried out by using the activation method for an enriched isotope; (2) measurements carried out by using the activation method for a natural elemental sample where the contribution from the heavier isotope is taken into account, including the present result; (3) measurements carried out by using the activation method for a natural elemental sample where the contribution from the heavier isotope is not taken into account: and (4) measurements carried out by detecting the outgoing charged particle. In cases where the measured cross sections from the same experiment have been reported more than once in different papers, only the measured data from the latest publication is plotted and only the literature from which these measured data are taken are kept in the list of references and cited in the text. The cross sections obtained by the TALYS-1.2 [5] nuclear model code with ldmodel1 are represented by a black dotted line, ldmodel2 by a blue dashed line, ldmodel3 by a green dashed-dotted line, ldmodel4 by a thick red solid line, ldmodel5 by a black dashed-dotted-dotted line, ENDF/B-VII.1 [16] cross sections by a thin black solid line, and JENDL-4.0 [17] by a thin green solid line. These notations are followed throughout in this paper.

A. The chromium isotopes

1. The ^{52}Cr$(n,p)^{52}$V reaction

Figure 1 shows the excitation function for the ^{52}Cr$(n,p)^{52}$V reaction. We can divide the measured cross sections into four groups: (1) measurements carried out by using the activation method for an enriched ^{52}Cr isotope [18–25]; (2) measurements carried out by using the activation method for a natural chromium sample [26–28] where the ^{53}Cr$(n,x)^{52}$V contribution is taken into account, including the present result; (3) measurements carried out by using the activation method for a natural chromium sample [29–43] where the ^{53}Cr$(n,x)^{52}$V contribution is not taken into account; and (4) measurements carried out by detecting the outgoing charged particle [44].

The measured γ energy and branching ratio used in the measurement are reported by all the authors in groups 1 and 2, which is 1.434 MeV and 100%, respectively, the same as the present case, while authors from group 3 reported the same or did not report the decay data. In the present paper, the cross section for the ^{52}Cr$(n,p)^{52}$V reaction is reported after subtracting the cross section of the ^{53}Cr$(n,x)^{52}$V reaction of 13.2 ± 1.04 mb at 14.87 MeV measured by Sakane *et al.* [45].

Below 9-MeV neutron energy, Smith *et al.* [23] and Manhart *et al.* [26] reported the measured cross sections. In this region, there is no contribution from the ^{53}Cr$(n,np)^{52}$V and ^{53}Cr$(n,d)^{52}$V reactions since the reaction threshold energies are 11.344 and 9.077 MeV, respectively. Hence measurements carried out using a natural sample of chromium gives a pure ^{52}Cr$(n,p)^{52}$V reaction cross section. We therefore include Smith *et al.*'s [23] measurements in group 1 here, although they used a natural chromium sample. It is clear from Fig. 1 that the measured cross sections agree very well with ENDF/B-VII.1 values and are in fair agreement with JENDL-4.0, TALYS-1.2 calculations with ldmodel1 and ldmodel4, whereas the

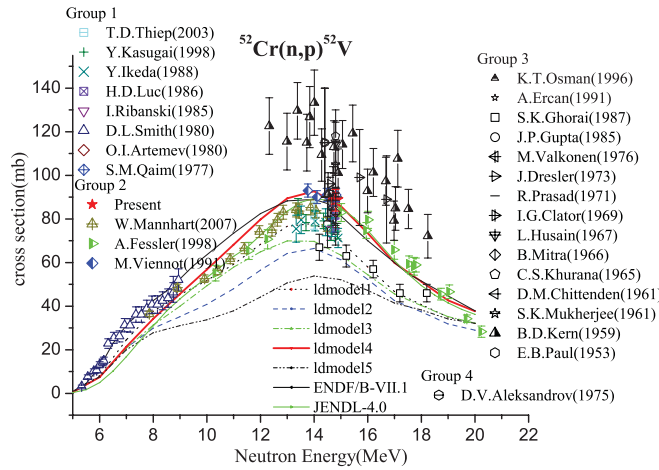

FIG. 1. (Color online) Excitation function of the ^{52}Cr$(n,p)^{52}$V reaction.

calculations with ldmodel2, ldmodel3, and ldmodel5 clearly underestimate the experimental cross sections.

Above 9 MeV, we observed an excellent agreement between measured data belonging to groups 1 and 2, the ENDF/B-VII.1, JENDL-4.0, and the TALYS-1.2 calculations with ldmodel4. It is worth mentioning that at around 14–15 MeV neutron energy where multiple measured data are available, the data from groups 1 and 2 agree with each other to within 10% whereas the data from groups 3 and 4 are either too high or too low and there is no consistent agreement among them. Our data at 14.8 MeV confirmed the data of Manhart *et al.* [26], Fessler *et al.* [27], and Viennot *et al.* [28]. Above 9-MeV incident neutron energy, all the measured cross sections very much above or below the evaluated cross-section values come from groups 3 and 4.

The TALYS-1.2 calculation with ldmodel1 is in excellent agreement with the experimental data below 12.5 MeV. It then follows Kasugai *et al.* [19], Ikeda *et al.* [20] data sets around 13–15 MeV, and is in excellent agreement with the data of Ghorai *et al.* [31] above 15 MeV. But data measured by Ghorai around 14 MeV deviate too much from all existing measured cross sections, and the true excitation curve does not seem to follow the trend of this particular data set, considering the fact that measured data below 12-MeV neutron energy are considered to be quite accurate and the contribution from the ^{53}Cr$(n,x)^{52}$V reaction is zero or negligibly small. The TALYS-1.2 calculations with ldmodel2, ldmodel3, and ldmodel5 clearly underestimate the experimental cross sections throughout the incident neutron energy range considered.

2. *The* ^{53}Cr$(n,p)^{53}$V *reaction*

Figure 2 shows the excitation function for the ^{53}Cr$(n,p)^{53}$V reaction. Dividing the measured data into groups as in the previous case: (1) measurements carried out by using the activation method for an enriched ^{53}Cr isotope [18,19,21,22,24,25,27,46]; (2) measurements carried out by using the activation method for a natural chromium sample where the ^{54}Cr$(n,x)^{53}$V contribution is taken into account—this group consists of only the present result; and (3) measurements carried out by using the activation method for a natural chromium sample [28–30,35,37,40,47–49] where the ^{54}Cr$(n,x)^{53}$V contribution is not taken into account.

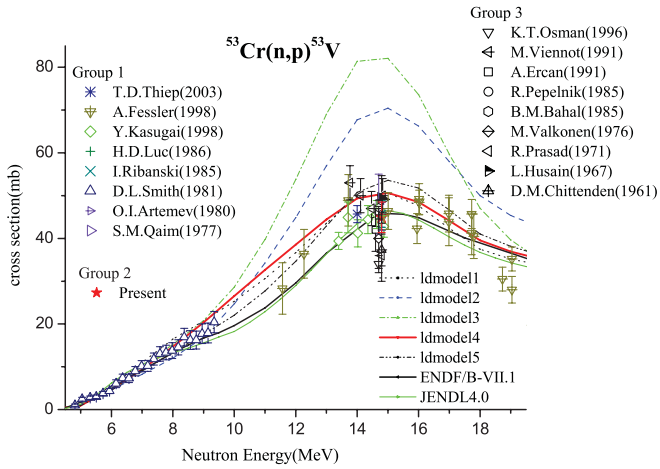

FIG. 2. (Color online) Excitation function of the ^{53}Cr$(n,p)^{53}$V reaction.

The measured γ energy and branching ratio used in the measurement are reported by all the authors, which is 1.006 MeV and 89.6%, the same as in the present case or 90%, respectively, except for Husain *et al.* [37], who reported 1.01 MeV and 100%, which is then normalized in the present paper, with respect to the latest decay probability of 89.6%. Artemev *et al.* [24], Ercan *et al.* [30], Prasad *et al.* [35], Chittenden *et al.* [40], and Pepelnik *et al.* [48] did not report the decay data.

In the present paper, the cross section for the ^{53}Cr$(n,p)^{53}$V reaction is reported after subtracting the cross section of the ^{54}Cr$(n,x)^{53}$V reaction of 3.0 ± 0.8 mb at 14.7-MeV incident energy measured by Qaim and Molla [25]. Below 9 MeV, there is excellent agreement between the measured data, the evaluated cross sections, and with all cross sections calculated using TALYS-1.2.

It can be clearly seen that at around 13–14 MeV, the data with higher values come from group 3. Above 9 MeV, we see excellent agreement between the evaluated cross sections and measured data, and fair agreement between measured data and TALYS-1.2 calculations with ldmodel1, ldmodel4, and ldmodel5. The results from the calculations with ldmodel2 and ldmodel3 are very much higher than all the other results. At 14.8 MeV, the present measured cross section confirmed the measured cross sections reported at the same neutron energy by Ribanski *et al.* [22], Artemev *et al.* [24], and Qaim *et al.* [25] from group 1. At the same incident energy at 14.8 MeV, the measured cross sections from group 3, reported by Viennot *et al.* [28] and Husain *et al.* [37], are higher by ∼7% than the present measured cross section, whereas the measured cross section reported by Chittenden *et al.* [40] is lower by ∼20% than the present measured cross section. The present measured cross section is also in excellent agreement with the evaluated data of ENDF/B-VII.1 and JENDL-4.0. The measured cross sections reported from group 3 are either too high or too low compared to the corresponding measured cross sections from groups 1 and 2, and the evaluated data of ENDF/B-VII.1 and JENDL-4.0.

B. The zinc isotopes

1. *The* ^{66}Zn$(n,p)^{66}$Cu *reactions*

Figure 3 shows the excitation function for the ^{66}Zn$(n,p)^{66}$Cu reaction. We again divided the measured cross sections into three groups: (1) measurements carried out by using the activation method for an enriched ^{66}Zn isotope [19,23,50]; (2) measurements carried out by using the activation method for a natural zinc sample [25,28,51] where the ^{67}Zn$(n,x)^{66}$Cu contribution is taken into account, including the present result; and (3) measurements carried out by using the activation method for a natural zinc sample [30,32,34–36,43,52–62] where the ^{67}Zn$(n,x)^{66}$Cu contribution is not taken into account.

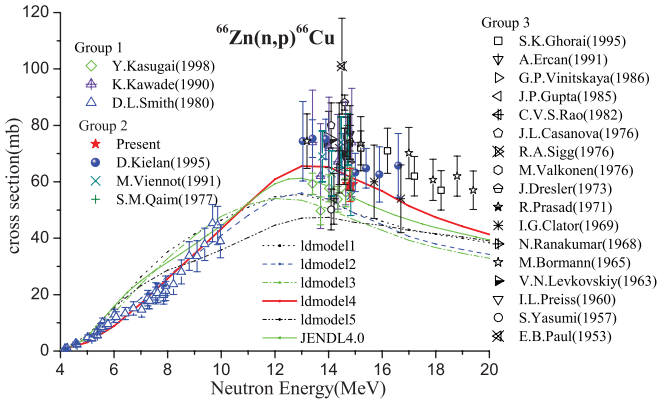

FIG. 3. (Color online) Excitation function of the ^{66}Zn$(n,p)^{66}$Cu reaction.

The measured γ energy and branching ratio used in the measurement are reported by all the authors in groups 1 and 2 except for Smith *et al.* [23]. Kasugai *et al.* [19] reported the same decay data as in the present paper, which is 9.23% for the 1.039-MeV γ-ray line, while Kawade *et al.* [50] and Kielan *et al.* [51] reported 7.4%, and Viennot *et al.* [28] and. Qaim *et al.* [25] reported 8% each for the same γ energy. We therefore normalized the data from groups 1 and 2 with respect to the latest γ branching ratio 9.23%, which is used in the present paper, and plotted again in Fig. 4 along with all the other data.

From group 3, Clator *et al.* [36], Rao *et al.* [54], Sigg *et al.* [56], and Ranakumar *et al.* [58] reported 9% for the same γ line, and the rest had not reported the decay data. Hence no normalization is done for group 3. In the present paper, the cross section for the ^{66}Zn$(n,p)^{66}$Cu reaction is reported after subtracting the cross section of the ^{67}Zn$(n,x)^{66}$Cu reactions of 35.9 ± 8.9 mb measured by Sakane *et al.* [45] at 14.8-MeV neutron energy.

After normalization, the present measured cross section and all the data from groups 1 and 2, at 14.8 MeV, agree within 2%. It is worth mentioning that at around 13–15 MeV neutron energy where multiple measured data is available, the data from groups 1 and 2 agree with each other within their

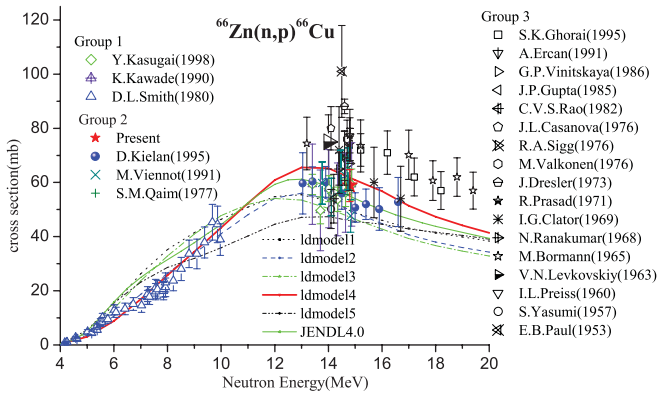

FIG. 4. (Color online) Excitation function of the ^{66}Zn$(n,p)^{66}$Cu reaction with the measured data of groups 1 and 2 normalized using the latest decay data [7].

experimental uncertainty, whereas the data from group 3 is too high compared to their corresponding data from groups 1 and 2.

The TALYS-1.2 calculations with ldmodel2 and ldmodel4 are in excellent agreement with the experimental data below 10 MeV, whereas the JENDL-4.0 and TALYS-1.2 calculations with ldmodel1, ldmodel3, and ldmodel5 overestimate the measured data. No experimental data are reported in the energy range 10–13 MeV. Above 13 MeV, the measured data from groups 1 and 2 are in excellent agreement with JENDL-4.0, the TALYS-1.2 calculation with ldmodel4 slightly overestimate these data, while all the other TALYS-1.2 calculations underestimate all the reported measured data.

2. *The* ^{68}Zn$(n,p)^{68}$Cu^m *reaction*

Figure 5 shows the excitation function for the ^{68}Zn$(n,p)^{68}$Cu^m reaction. It is observed from Fig. 5 that measured cross sections have been reported only in the energy range 13–16 MeV. All the authors [8,28,30,48,50–52,54–56, 60,63,64] reported data within less than 2.2% of the measured γ energy branching ratio used in the present paper, for a 0.525-MeV γ ray, except for Kielan *et al.* [51], who reported 12.9% for a 1.077-MeV γ line; the latest value is 12%, and normalization would then increase the reported cross section by 7.5%. Rao *et al.* [54] reported 68% for an 84-keV γ-ray line while the latest data is 70% for this γ line, and normalization would then decrease this cross section by 3%. The original reported cross sections, and not the normalized ones, are plotted. Ercan *et al.* [30], Pepelnik *et al.* [48], Casanova *et al.* [55], Levkovskiy *et al.* [60], and Tikku *et al.* [64] did not report decay data.

From Fig. 5, in the energy region 13–15 MeV, TALYS-1.2 calculations with ldmodels 1, 2, 3, and 5 overestimate the measured cross sections by more than 60%, and the ldmodel4 calculation slightly overestimates the measured cross sections

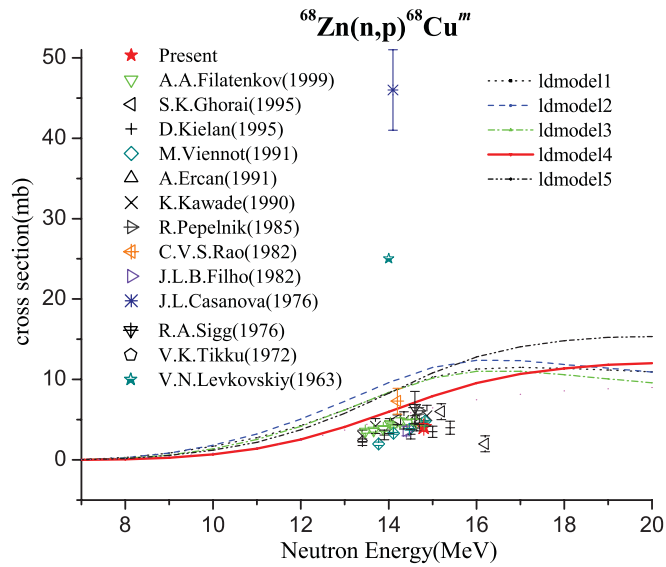

FIG. 5. (Color online) Excitation function of the ^{68}Zn$(n,p)^{68}$Cu^m reaction.

while reproducing the trend of the measured cross sections. The shape of the excitation curve above 15 MeV cannot be confirmed since there is only one experimental point. The cross sections reported by Casanova *et al.* [55] and Levkovskiy *et al.* [60] are clearly not the cross sections of interest, and it is possible that the reported data are ^{68}Zn$(n,p)^{68}$Cu^{m+g} and ^{68}Zn$(n,p)^{68}$Cu^{g} cross sections, respectively. Since no decay data are given by these authors, we cannot confirm this, though.

C. The ^{97}Mo$(n,p)^{97}$Nb^m and ^{97}Mo$(n,p)^{97}$Nb^g reactions

Figure 6 shows the excitation function for the ^{97}Mo$(n,p)^{97}$Nb^m reaction. Again dividing the measured data into groups, (1) measurements were carried out by using the activation method for an enriched ^{97}Mo isotope (Reimer *et al.* [3], Kasugai *et al.* [19], Ikeda *et al.* [20], and Artemev *et al.* [24]), (2) measurements were carried out by using the activation method for a natural molybdenum sample where the ^{98}Mo$(n,x)^{97}$Nb^m contribution is taken into account, including the present result (Reimer *et al.* [3], Bostan *et al.* [65], Marcinkowski *et al.* [66], and Amemiya *et al.* [67]), and (3) measurements were carried out by using the activation method for a natural molybdenum sample where the ^{98}Mo$(n,x)^{97}$Nb^m contribution is not taken into account (Gueltekin *et al.* [68], Rao *et al.* [69], and Lu *et al.* [70]).

In the present paper, the cross section for the ^{97}Mo$(n,p)^{97}$Nb^m reaction is reported after subtracting the cross section of the ^{98}Mo$(n,x)^{97}$Nb^m reactions of 0.84 ± 0.20 mb measured by Amemiya *et al.* [67] at 14.8-MeV neutron energy.

All authors reported basically the same decay data as the present paper, except for Reimer *et al.* [3], Artemev *et al.* [24], and Gueltekin *et al.* [68], who did not report decay data. At 14.8 MeV, our result confirmed the measurement of Amemiya *et al.* [67] from group 2, who reported 4.3 ± 1.0 mb. In the energy region between 13 and 15 MeV, agreement between different measured data is very good within their experimental uncertainty, except for Lu from group 3's data and Artemev

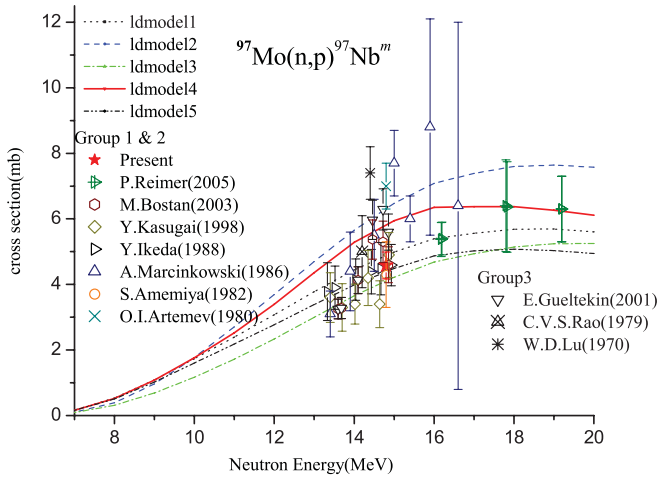

FIG. 6. (Color online) Excitation function of the ^{97}Mo$(n,p)^{97}$Nb^m reaction.

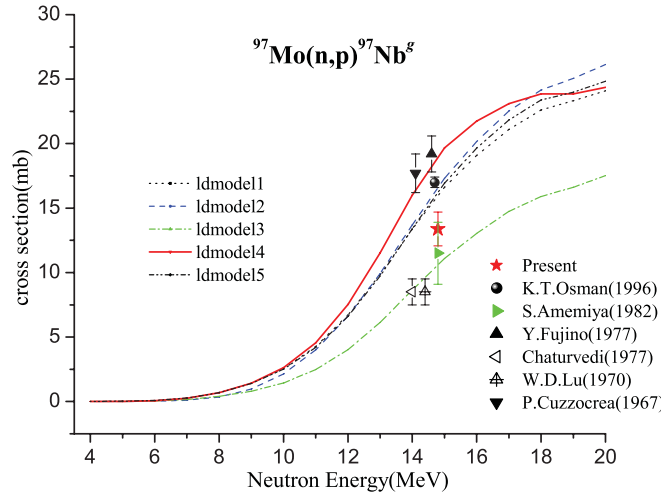

FIG. 7. (Color online) Excitation of the ^{97}Mo$(n,p)^{97}$Nb^g reaction.

from group 1's data, which are more than 50% higher than the other measured data. Artemev's data, though belonging to group 1, cannot be confirmed since the decay data and percent enrichment of the isotope is not given. It is also interesting to see that the data of Kasugai *et al.* [19] and Ikeda *et al.* [20] show a much slower increase compared to the data reported by Marcinkowski *et al.* [66]. The shapes of the excitation curves of the TALYS-1.2 calculation also exhibit a trend similar to the Kasugai and Ikeda data sets.

Between 13 and 15 MeV, the TALYS-1.2 calculations with ldmodel 1, 3, and 5 agree very well with measured data within reported data uncertainty, while the TALYS-1.2 calculation with ldmodel 4 slightly overestimates the measured data. The calculated cross section with ldmodel2 is very high compared to measured data throughout the excitation curve.

Figure 7 shows the excitation function for ^{97}Mo$(n,p)^{97}$Nb^g reaction. It is observed that very few measured cross sections have been reported around 14 MeV. Moreover, large discrepancies exist between the measured cross sections. It is therefore important to look carefully at the literature and study the measurement processes employed.

The isomeric level of 0.743 MeV undergoes a 100% internal transition (IT) to the ground state with a 58.7-s half-life. The unstable ground state having a half-life of 72.1 min then undergoes a β decay with 100% probability. The γ line of energy 0.658 MeV with a branching ratio of 98.23% originating from the β-decay daughter nucleus (^{97}Mo) is then measured. It is therefore very important to subtract the contribution of the metastable state to the unstable ground state in order to determine the ^{97}Mo$(n,p)^{97}$Nb^g cross section. At the same time, it is very important to wait and cool for a sufficient time to allow the metastable state to completely decay to the ground state if we are to measure the ^{97}Mo$(n,p)^{97}$Nb total cross section. In our measurement, we measure the activity immediately after the sample irradiation; the cooling time was just 20 s. Hence, to obtain a pure ^{97}Mo$(n,p)^{97}$Nb^g cross section, we apply correction for the contribution of the metastable state as described in Ref. [67], as well as the correction from the contribution of ^{98}Mo$(n,x)^{97}$Nb^g of 1.5 ± 0.3 mb measured by Amemiya *et al.* [67] at 14.8-MeV neutron

energy. The literature survey for the measured data plotted in Fig. 7 reveals that only Amemiya *et al.*'s measurement satisfies the above procedure. Our measured data also agree with the cross section reported by Amemiya *et al.* [67]. All authors [29,67,70–73] reported the same γ line energy and branching ratio used in the present paper, except for Chaturvedi *et al.* [71], who had not reported the decay data.

The TALYS-1.2 calculation with ldmodel3 agrees fairly well with our result and the cross section reported by Amemiya *et al.* [67], whereas the other TALYS-1.2 calculations overestimate our result and the cross sections reported by Amemiya, Lu, and Chaturvedi.

D. The tin isotopes

1. *The* ^{116}Sn$(n,p)^{116}$In^{m1+m2} *reaction*

It is observed from Fig. 8 that there are only four measured cross sections reported in the literature, over the neutron energy range considered in the present paper, for the ^{116}Sn$(n,p)^{116}$In^{m1+m2} reaction. In the present paper, the contribution of the ^{117}Sn$(n,np)^{116}$In^{m1+m2} reaction, measured by Ikeda *et al.* [20] of 1.38 $\pm$ 0.17 mb at 14.72-MeV neutron energy, has been subtracted.

Lulic *et al.* [74] used a 92.8% enriched sample, and Brzosko *et al.* [75] did not report the degree of enrichment. Struwe *et al.* [76] and Chursin *et al.* [77] used natural tin samples, and no correction from a higher isotope contribution is reported. The measured decay γ energy and its disintegration probability reported by Struwe *et al.* [76] are 1.290 MeV and 82%, respectively. Hence, these data are normalized with respect to the decay data used in the present paper. The other three authors did not report the decay data. In the present paper, we measured the activity of two decay γ's, 0.417 MeV with 27.2% intensity and 1.293 MeV with 84.8% intensity. The reported cross section is the average of the cross sections estimated with the activity of these two γ-ray lines.

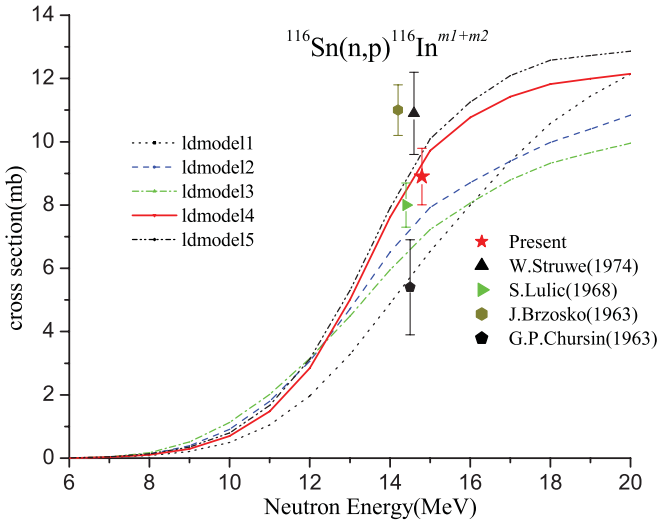

FIG. 8. (Color online) Excitation function of the ^{116}Sn$(n,p)^{116}$In^{m1+m2} reaction.

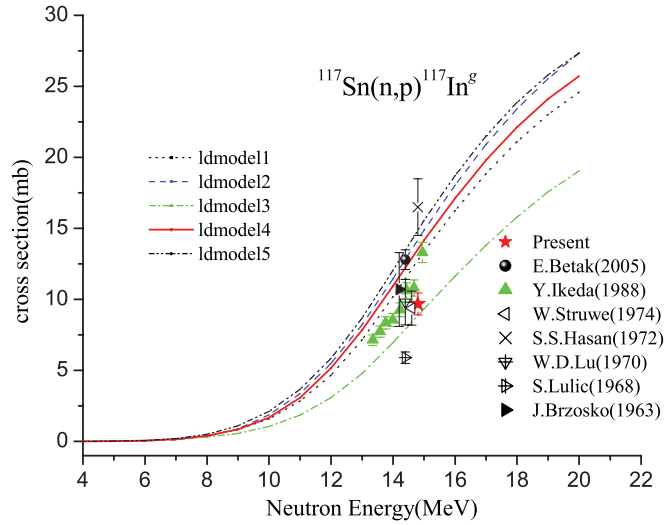

FIG. 9. (Color online) Excitation function of the ^{117}Sn$(n,p)^{117}$In^{g} reaction.

The theoretical values of the cross sections estimated in the present paper with the choice of ldmodel4 and ldmodel5 are in good agreement with the present result and Lulic's data, whereas the other TALYS-1.2 results are very much below these two experimental points.

2. *The* ^{117}Sn$(n,p)^{117}$In^{g} *reaction*

Figure 9 shows the excitation function for the ^{117}Sn$(n,p)^{117}$In^{g} reaction. There have been seven measured data points around 14 MeV reported in the literature.

The isomeric and ground-state information about the residual nucleus ^{117}In is given in Table III. The isomeric state decays by beta emission by 52.90% while it undergoes an internal transition to the ground state by 47.10%. Hence, ideally the isomeric state contribution has to be subtracted for this reaction. But for the fact that it feeds the ground state with 47.10% disintegration probability, the half-life of the isomeric state (116.2 min [7]) being 2.7 times larger than the ground-state half-life, and the times for sample irradiation, cooling, and counting times being 5, 1.28, and 5 min, respectively, the isomeric state contribution to the ground-state formation is expected to be very small. Therefore, in the present paper, only the ^{118}Sn$(n,x)^{117}$In^{g} contribution is taken into account during the analysis. None of the authors in Fig. 9 reported taking this interference into account. The contribution of ^{118}Sn$(n,x)^{117}$In^{g} measured by Brzosko of 0.93 $\pm$ 0.26 mb [78] at 14.9-MeV neutron energy has been subtracted in the present paper.

TABLE III. Isomeric and ground state information of ^{117}In [7].

Level (MeV)	J^{π}	Δ (MeV)	$T_{1/2}$ (min)	Decay modes
0.0	$9/2^{+}$	−88.9450	43.2	β^{-}: 100.00%
0.3153	$1/2^{-}$	−88.6297	116.2	β^{-}: 52.90%
				IT: 47.10%

Ikeda *et al.* [20] and Lulic *et al.* [74] used an enriched ^{117}Sn isotope in their measurement, with the latter reporting 85.4% enrichment. The decay data for the measured 0.553-MeV γ-ray line reported by Ikeda *et al.* [20], Lu *et al.* [70], and Betak *et al.* [79] are the same as the present paper, while Struwe *et al.* [76] reported a 95.7% disintegration probability for the 0.553-MeV γ-ray line, and hence normalization with respect to the present decay data is performed for this particular data point and plotted. Brzosko *et al.* [75] and Hasan *et al.* [80] did not report the decay data. Our result agrees well with Ikeda's data at 14.76 MeV while Hasan's measured data at 14.8 MeV is higher by ∼70%. The measured data of Lu at 14.4 MeV is also lower by ∼ 44% than the other reported data at the same energy. The cross sections measured by Ikeda *et al.* [20], Brzosco *et al.* [75], Struwe *et al.* [76], and Lu *et al.* [70] all lie within the TALYS-1.2 calculation with ldmodel 3 and 4.

3. *The* ^{118}Sn$(n,p)^{118}$In^{m1+m2} *reaction*

Figure 10 shows the excitation function for the ^{118}Sn$(n,p)^{118}$In^{m1+m2} reaction. There are very few reported measured cross sections around 14 MeV. Moreover, there is a large discrepancy between the measured cross sections. Murahira *et al.* [81] reported six data points between 13 and 15 MeV, and Struwe *et al.* [76] and Chursin *et al.* [77] reported a single data point each. Murahira *et al.* [81] reported their measured decay γ-ray line 0.683 MeV with 55%, which is the same as the present paper; Struwe *et al.* [76] reported their measured decay γ-ray line of 1.229 MeV with a 96% disintegration probability, which is the same as the latest decay data in Nudat-2.5 [7], while Chursin *et al.* [77] had not reported the decay data. Furthermore, none of the authors reported the correction for the ^{119}Sn$(n,x)^{118}$In^{m1+m2} contribution. We have not corrected the ^{119}Sn$(n,x)^{118}$In^{m1+m2} contribution either since no measured data are reported for this reaction.

It is clear from Fig. 10 that there is a large discrepancy between the measured data reported by Murahira *et al.* [81]

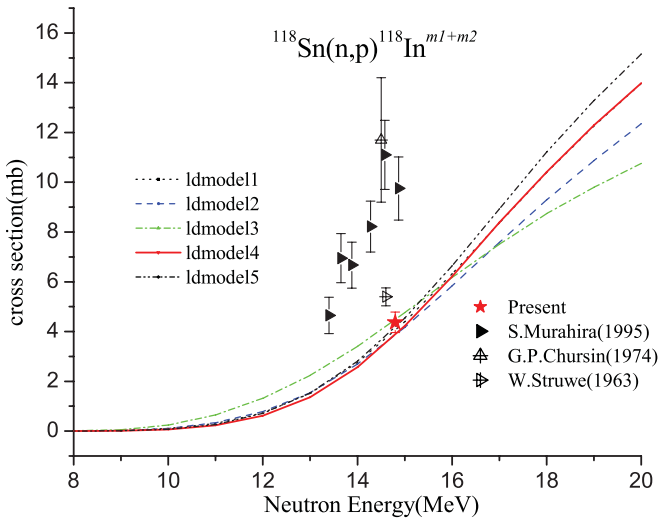

FIG. 10. (Color online) Excitation function of the ^{118}Sn$(n,p)^{118}$In^{m1+m2} reaction.

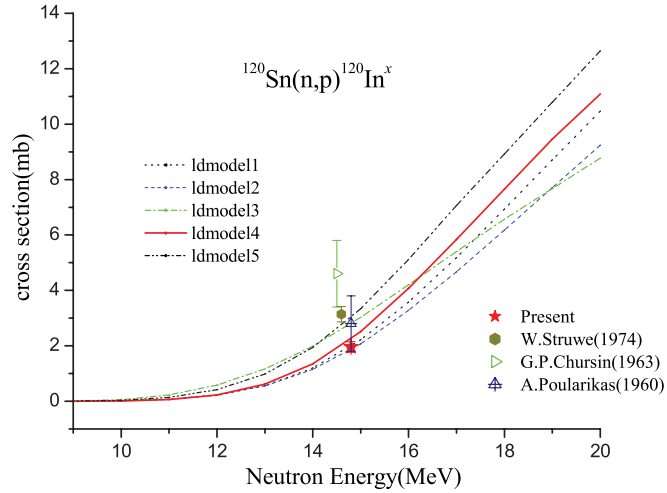

FIG. 11. (Color online) Excitation function of the ^{120}Sn$(n,p)^{120}$In^{x} reaction.

and Chursin *et al.* [77] with the measured data reported by Struwe *et al.* [76] and the present result. The discrepancy is more than 100% at their corresponding energies. In the TALYS-1.2 calculation, ^{118}Sn$(n,p)^{118}$In^{m1} and ^{118}Sn$(n,p)^{118}$In^{m2} cross sections are added and plotted in Fig. 10. It is interesting to see that all the TALYS-1.2 calculations agree very well below 16 MeV. The present result is in excellent agreement with all the TALYS-1.2 calculations, and Struwe's data is very close to the theoretical predictions, whereas the data reported by Murahira and Chursin are clearly too high.

4. *The* ^{120}Sn$(n,p)^{120}$In^{x} *reaction*

Figure 11 shows the excitation function for the ^{120}Sn$(n,p)^{120}$In^{x} reaction. A γ-ray line of energy 1.171 MeV is emitted by ^{120}Sn, through the three levels given in Table IV, undergoing a β decay from ^{120}In. A literature review on the history of these three states in the nuclear decay and structure data library (ENSDF) indicates that the following: Until 1976, two levels [3.08 s 1^+ and 44.4 s $(5)^+$] were given, but the ordering of the two levels was unknown [82], until 1987, three levels [3.08 s 1^+, 46.2 s $(5)^+$, and 47.3 s (8^-)] were given, but the ordering of the three levels was unknown [83]; and until 2002, three levels [3.08 s 1^+, 47.3 s (8^-), and 46.2 s $(5)^+$] were given. The ordering of the two levels (1^+ and 8^-) was unknown [84]. Therefore, we did not know which one of these three states was the ground state before 2002, and we still do not know which one of the two states (1^+ and 8^-) is the ground state.

TABLE IV. Isomeric and ground-state information of ^{120}In [7].

E (level) (MeV)	J^π	Δ (MeV)	$T_{1/2}$ (min)	Decay modes
0.0	1^+	−85.7351	3.08 s	β^-: 100%
$0.0+x$	8^-	−85.7351	47.3 s	β^-: 100%
0.0700	5^+	−85.6651	46.2 s	β^-: 100%

According to Nudat-2.5 [7], the β-delayed γ-ray line from ^{120}In (0.051 min, 1^+) of energy 1.1725 MeV with 19% intensity, from ^{120}In (0.788 min, 8^-) of energy 1.1712 MeV with 100% intensity, and from ^{120}In (0.77 min, 5^+) of energy 1.1712 MeV with 97% intensity, respectively, are known. Hence with the two levels having almost the same half-life, and both of them undergoing a β decay with ~100% probability, it is therefore difficult to distinguish between state 8^- ($T_{1/2} = 47.3$ s) and metastable state 5^+ ($T_{1/2} = 46.2$ s) by measuring the 1.171-MeV decay γ. In the present paper, we measured the γ ray of energy 1.171 MeV and used 100% as its intensity in our analysis, and called our measured cross section ^{nat}Sn$(n,x)^{120}$In^x. Note that the 1^+ state contribution was negligible because its half-life (0.051 min) is five times shorter than the cooling time (0.25 min).

In Fig. 11, Chursin *et al.* [77] and Poularikas *et al.* [85] reported half-lives of 51 and 50 s, respectively, and they did not report their measured γ-ray energy and its intensity, while Struwe *et al.* [76] reported 1.169 MeV with 95% intensity and a half-life of 45.4 s in their measurement. All these measurements were performed and reported before 1976.

The discrete level scheme adopted for ^{120}In in TALYS-1.2 has two levels, (0.051 min, 1^+) and (0.770 min, 5^+). The level (0.778 min, 8^-) is missing. Hence, we updated the ^{120}In discrete level scheme and included the (0.778 min, 8^-) level. The plotted TALYS-1.2 cross-section values in Fig. 11 are the sum of the (0.770 min, 5^+) and (0.778 min, 8^-) states' production cross section. It is observed from Fig. 11 that our measured cross section at 14.8 MeV in the present paper is in excellent agreement with the TALYS-1.2 theoretical cross-section values obtained with the choices of ldmodel 1, 2, and 4. It is worth mentioning that the cross section reported by Chursin *et al.* [77] is consistently much higher in the ^{118}Sn$(n,p)^{118}$In^{m1+m2} and ^{120}Sn$(n,p)^{120}$In^x reactions than all the theoretical and reported measured cross sections.

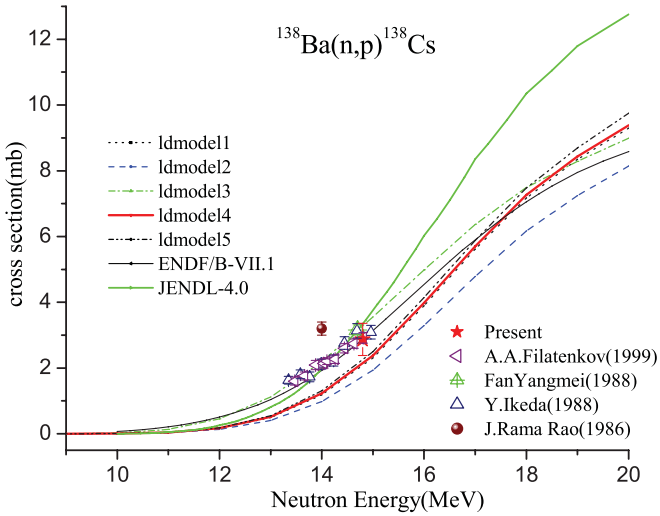

FIG. 12. (Color online) Excitation function for ^{138}Ba$(n,p)^{138}$Cs reaction.

E. The ^{138}Ba$(n,p)^{138}$Cs reaction

Figure 12 shows the excitation function for the ^{138}Ba$(n,p)^{138}$Cs reaction. It is observed that there are two sets of measured data between 13 and 15 MeV reported by Filatenkov *et al.* [8] and Ikeda *et al.* [20], and a single data point each by Fan *et al.* [86] and Rao *et al.* [87]. Ikeda *et al.* [20] reported their measured decay γ energy of 1.435 MeV, which is the same as the present paper, with 75% intensity, while others did not report the decay data in their measurement. The measured data reported by Rao is clearly much higher than all the reported data and TALYS-1.2 calculations at the corresponding energy. We observed an excellent agreement between all other measured data—ENDF/B-VII.1 and JENDL-4.0—with the present result. The agreement between the ENDF/B-VII.1 and ldmodel3 calculations is good throughout the energy range considered. The TALYS-1.2 calculation with ldmodel 4 and 5 underestimates the measured cross sections as well as the evaluated cross sections below 16 MeV, and the agreement then improves as the energy increases. The TALYS-1.2 calculation with ldmodel2 underestimates the measured cross sections and is too much below all the other theoretical values and evaluated cross sections throughout the energy range 0–20 MeV. Similarly, JENDL-4.0 agrees very well below 15 MeV and increases monotonically above 15 MeV, and clearly is very much above ENDF/B-VII.1 and all the TALYS-1.2 calculations as the incident energy increases.

V. SUMMARY AND CONCLUSIONS:

A set of reaction cross-section measurements, in comparison with previously reported measured cross sections and TALYS-1.2 nuclear model calculations with different level density models, have been performed. A consistent trend observed is that measured data from group 1 (measurements carried out by using the activation method for an enriched isotope) and group 2 [measurements carried out by using the activation method for a natural sample where the (n,x) contribution from the heavier isotope is taken into account, including the present result] consistently agree with each other within their experimental uncertainty, whereas the measured data from group 3 [measurements carried out by using the activation method for a natural sample where the (n,x) contribution from the heavier isotope is not taken into account] and group 4 (measurements carried out by detecting the outgoing charged particle) are much higher or lower and inconsistent among themselves. Another systematic observation is the decreasing trend of the cross section with an increasing mass number for isotopes.

The cross sections for (n,p) reactions with different isotopes of the same element (Table V) reveal that the neutron cross section decreases with an increase in the neutron number. The variations in the cross section with isotopes were studied by a few authors [8,88–92]. In the present paper, this isotopic effect is observed for chromium and tin isotopes in which the (n,p) cross section decreases with neutron number at all of the neutron energies considered. This can be explained in terms of an increase in the cross section of the (n,n') and $(n,2n)$ reaction and hence a decrease in the (n,p) cross section. Moreover, the threshold of the (n,p) reaction also increases with neutron

TABLE V. The present measured cross sections of the (n,p) reactions at 14.8-MeV neutron energy. The second column is obtained from Eq. (1), the fourth column is obtained from Eq. (3), and the last column is obtained from Eq. (4). Italicized cross sections are corrected for interferences of heavier isotopes in the sample target by subtraction of cross sections in literature.

Measured reaction	Measured elemental cross section (mb)	(n,p) reaction	Corrected (n,p) isotopic cross section (mb)	Subtracted literature $(n,np)+(n,d)$ isotopic cross section (mb)	Uncorrected (n,p) isotopic cross section (mb)
$^{nat}Cr(n,x)^{52}V$	75.47 ± 4.22	$^{52}Cr(n,p)^{52}V$	88.57 ± 4.95	13.20 ± 1.04 [45]	90.07 ± 5.04
$^{nat}Cr(n,x)^{53}V$	4.27 ± 0.34	$^{53}Cr(n,p)^{53}V$	44.95 ± 3.58	(no subtraction)	44.95 ± 3.58
$^{nat}Zn(n,x)^{66}Cu$	17.89 ± 1.79	$^{66}Zn(n,p)^{66}Cu$	58.85 ± 5.89	35.90 ± 8.90 [45]	64.12 ± 6.41
$^{nat}Zn(n,x)^{68}Cu^{m}$	0.76 ± 0.09	$^{68}Zn(n,p)^{68}Cu^{m}$	4.05 ± 0.48	(no subtraction)	4.05 ± 0.48
$^{nat}Mo(n,x)^{97}Nb^{g}$	1.64 ± 0.16	$^{97}Mo(n,p)^{97}Nb^{g}$	13.38 ± 1.31	1.50 ± 0.30 [67]	17.17 ± 1.67
$^{nat}Mo(n,x)^{97}Nb^{m}$	0.64 ± 0.06	$^{97}Mo(n,p)^{97}Nb^{m}$	4.58 ± 0.43	0.84 ± 0.20 [67]	6.70 ± 0.63
$^{nat}Sn(n,x)^{116}In^{m1+m2}$	1.40 ± 0.14	$^{116}Sn(n,p)^{116}In^{m1+m2}$	8.90 ± 0.89	1.38 ± 0.17 [20]	9.63 ± 0.96
$^{nat}Sn(n,x)^{117}In^{g}$	0.97 ± 0.08	$^{117}Sn(n,p)^{117}In^{g}$	9.69 ± 0.79	0.93 ± 0.26 [78]	12.63 ± 1.04
$^{nat}Sn(n,x)^{118}In^{m1+m2}$	1.06 ± 0.10	$^{118}Sn(n,p)^{118}In^{m1+m2}$	4.38 ± 0.41	(no subtraction)	4.38 ± 0.41
$^{nat}Sn(n,x)^{120}In^{x}$	0.64 ± 0.06	$^{120}Sn(n,p)^{120}In^{x}$	1.96 ± 0.18	(no subtraction)	1.96 ± 0.18
$^{nat}Ba(n,p)^{138}Cs$	2.06 ± 0.35	$^{138}Ba(n,p)^{138}Cs$	2.87 ± 0.49	(no subtraction)	2.87 ± 0.49

number due to a change in the Q value. This Q-value effect can be used to explain the decrease in the cross section of the (n,p) reaction for even A tin isotopes considered in the present paper. However, in the case of chromium isotopes considered in the present paper, the Q values of the reactions $^{52}Cr(n,p)^{52}V$ and $^{53}Cr(n,p)^{53}V$ are -3.193 and -2.653 MeV, respectively. The decrease in the (n,p) cross section with neutron number in the case of chromium isotopes and in the case of ^{117}Sn, although their Q value increases, can be explained on the basis of the level densities of the final nuclei due to the pairing energy.

In the case of the $^{52}Cr(n,p)^{52}V$ reaction, after emission of a proton, the nucleus becomes odd-odd. However, in the case of neutron emission, the nucleus is even-even. In the case of the $^{53}Cr(n,p)^{53}V$ reaction, the residual nucleus produced after emission of a proton or a neutron becomes odd-even or even-odd, respectively. Thus the level densities act strongly to the advantage of proton emission from the reaction of neutrons with the even-even chromium isotope and in disfavor of emission of protons from the reactions with the odd-mass chromium isotope [92]. Therefore, in the case of chromium, the level densities compensate for the advantage of the lower Q value and result in a decrease in the cross section for the $^{53}Cr(n,p)^{53}V$ reaction. The same argument is true for the decrease in the (n,p) reaction cross section for the odd A tin isotope considered in the present paper. The decrease of cross sections with an increase in the neutron number in the target nuclei can also be explained based on the fact that (n,p) reactions are less favored for the more neutron-rich isotopes, because the reaction product is even more neutron rich.

In conclusion, in the present paper, a careful and systematic set of experiments has been carried out, and (n,p) reaction cross sections have been measured and determined with relatively small uncertainties, using the latest decay data, and by taking into account the contributions from heavier isotopes and the contribution of metastable states in the case of unstable ground-state formation cross sections. A systematic study and careful comparison of previously reported measured cross sections with the newly measured data reveals that the discrepancies among the previously reported measured data are due to (1) decay data used in the experimental determination of the cross sections, (2) contributions from the heavier isotopes present in the irradiated sample, and (3) contributions from metastable states in the case of unstable ground-state formation cross sections. We believe and hope that these new sets of measured data can help in fixing statistical model parameters to understand these reactions in terms of statistical models and to a better evaluation of these reaction cross sections in the future.

ACKNOWLEDGMENTS

This work was carried out under the joint collaboration research program between the University of Pune and BARC, Mumbai. For this work the financial support provided by the B.R.N.S., DAE, Mumbai, under a research project is gratefully acknowledged. B.L. and N.O. are grateful to H. Naik, Radiochemistry Division, Bhabha Atomic Research Centre, Mumbai, and R. Forrest, IAEA Nuclear Data Section, Vienna, for a careful review of the manuscript and for their valuable suggestions. N.O. is also indebted to V. Semkova, IAEA Nuclear Data section, Vienna, for her valuable comments.

[1] K. Kondo, S. Takagi, I. Murata *et al.*, Fusion Eng. Des. **81**, 1527 (2006).
[2] S. Ganesan, Pramana **68**, 257 (2007).
[3] P. Reimer, V. Avrigeanu, S. V. Chuvaev *et al.*, Phys. Rev. C **71**, 044617 (2005).
[4] EXFOR Nuclear Reaction Data Library, [http://www-nds.iaea.org/exfor/].
[5] A. J. Koning, S. Hilaire and M. Duijvestijn, "TALYS-1.0, A nuclear reaction program," NRG-1755 ZG Petten, The Netherlands, 2008, [http://www.talys.eu].

[6] M. I. Abbas, J. Phys. D: Appl. Phys. **39**, 3952 (2006).
[7] Nudat-2.5, NNDC BNL database, [http://www.nndc.bnl.gov].
[8] A. A. Filatenkov, S. V. Chuvaev, V. N. Aksenov *et al.*, Khlopin Radiev. Institute, Leningrad, Report No. 252, 1999 (unpublished).
[9] J. Csikai, in *Proceedings of the International Conference on Nuclear Data for Science and Technology*, Antwerp, 1982 (Reidel, Dordrecht, 1983), p. 414.
[10] L. F. Curtiss, *Introduction to Neutron Physics* (Van Nostrand, Princeton, NJ, 1969).
[11] A. J. Koning and J. P. Delaroche, Nucl. Phys. A **713**, 231 (2003).
[12] S. Watanabe, Nucl. Phys. **8**, 484 (1958).
[13] W. Hauser and H. Feshbach, Phys. Rev. **87**, 366 (1952).
[14] C. Kalbach, Phys. Rev. C **33**, 818 (1986).
[15] RIPL-2 Reference Input Parameter Library, IAEA, A-1400 Vienna, IAEA-NDS, [http://www-nds.iaea.org/RIPL-2/].
[16] M. B. Chadwick, M. Herman, P. Oblozinsky *et al.*, Nucl. Data Sheets **112**, 2887 (2011).
[17] K. Shibata, O. Iwamoto, T. Nakagawa, N. Iwamoto, A. Ichihara, S. Kunieda, S. Chiba, K. Furutaka, N. Otuka, T. Ohsawa, T. Murata, H. Matsunobu, A. Zukeran, S. Kamada, and J. Katakura, J. Nucl. Sci. Technol. **48**, 1 (2011).
[18] Tran Due Thiep, Nguyen Van Do, Truong Thi An, and Nguyen Ngoc Sona, Nucl. Phys. A **722**, 568 (2003).
[19] Y. Kasugai, H. Yamamoto, K. Kawade, and T. Iida, Ann. Nucl. Ener. **25**, 23 (1998).
[20] Y. Ikeda, C. Konno, K. Oishi, T. Nakamura, H. Miyade, K. Kawade, H. Yamamoto, and T. Katoh, JAERI, Report No.1312, 1988 (unpublished).
[21] Hoang Dac Luc, Phan Nhu Ngoc, Nguyen Van Do, and Ly Ba Bach, International Atomic Energy Agency, Report No. INDC(VN)-5, 1986 (unpublished).
[22] I. Ribansky, Ts. Panteleev, and L. Stoeva, Ann. Nucl. Energy **12**, 577 (1985).
[23] D. L. Smith and J. W. Meadows, Nucl. Sci. Eng. **76**, 43 (1980).
[24] O. I. Artem'ev, I. V. Kazachevskiy, V. N. Levkovskiy, V. L. Poznyak, and V. F. Reutov, At. Energ. **49**, 195 (1980).
[25] S. M. Qaim and N. I. Molla, Nucl. Phys. A **283**, 269 (1977).
[26] W. Mannhart and D. Schmidt, Phys. Techn. Bundesanst., Neutronenphysik Report No. PTB-N-53, 2007 (unpublished).
[27] A. Fessler, E. Wattecamps, D. L. Smith, and S. M. Qaim, Phys. Rev. C **58**, 996 (1998).
[28] M. Viennot, M. Berrada, G. Paic, and S. Joly, Nucl. Sci. Eng. **108**, 289 (1991).
[29] K. T. Osman and F. I. Habbani, International Atomic Energy Agency, Report No. INDC(SUD)-001, 1996 (unpublished).
[30] A. Ercan, M. N. Erduran, M. Subasi, E. Gueltekin, G. Tarcan, A. Baykal, and M. Bostan, in *Proceedings of the Conference on Nuclear Data for Science and Technology*, Juelich (Springer, Berlin, 1991), p. 376.
[31] S. K. Ghorai, J. R. Williams, and W. L. Alford, J. Phys. G **13**, 405 (1987).
[32] J. P. Gupta, H. D. Bhardwaj, and R. Prasad, Pramana **24**, 637 (1985).
[33] M. Valkonen, P. Homberg, R. Rieppo, J. K. Keinaenen, and J. Kantele, Phys. Lett. B **39**, 625 (1972).
[34] J. Dresler, J. Araminowicz, and U. Garuska, Prog. Rep.: Inst. Badan Jadr. (Nucl. Res.), Swierk+Warsaw, Report No. INR-1464, 1973, p. 12 (unpublished).
[35] R. Prasad and D. C. Sarkar, Nuovo Cimento A **3**, 467 (1971).
[36] I. G. Clator, Diss. Abstr. Int., B **30**, 2850 (1969).
[37] L. Husain and P. K. Kuroda, J. Inorg. Nucl. Chem. **29**, 2665 (1967).
[38] B. Mitra and A. M. Ghose, Nucl. Phys. **83**, 157 (1966).
[39] C. S. Khurana and I. M. Govil, Nucl. Phys. **69**, 153 (1965).
[40] D. M. Chittenden and D. G. Gardner, University of Arkansas Progress Report, Report No. 61, 1961, p. 1 (unpublished).
[41] S. K. Mukherjee, A. K. Ganguly, and N. K. Majumder, Proc. Phys. Soc. (London) **77**, 508 (1961).
[42] B. D. Kern, W. E. Thompson, and J. M. Ferguson, Nucl. Phys. **10**, 226 (1959).
[43] E. B. Paul and R. L. Clarke, Can. J. Phys. **31**, 267 (1953).
[44] D. V. Aleksandrov, L. I. Klochkova, and B. S. Kovrigin, At. Energ. **39**, 137 (1975).
[45] H. Sakane, K. Y. Kasugai, M. Shibata, T. Iida, A. Takahashi, T. Fukahori, and K. Kawade, Ann. Nucl. Eng. **29**, 53 (2002).
[46] D. L. Smith, J. W. Meadows, and F. F. Porta, Nucl. Sci. Eng. **78**, 420 (1981).
[47] M. Valkonen, P. Homberg, R. Rieppo, J. K. Keinaenen, and J. Kantele, J. Inorg. Nucl. Chem. **36**, 715 (1974).
[48] R. Pepelnik, B. Anders, and B. M. Bahal, in *Proceedings of the International Conference on Nuclear Data for Basic and Applied Science*, Santa Fe, 1985 (Gordon and Breach, New York, 1986), Vol. 1, p. 211.
[49] B. M. Bahal and R. Pepelnik, Ges. Kernen.-Verwertung, Schiffbau and Schiffahrt, Report No. GKSS-85-E, 1985, p. 11 (unpublished).
[50] K. Kawade, H. Yamamoto, T. Yamada, T. Katoh, T. Iida, and A. Takahashi, NEANDC(J), Report No. 154, 1990 (unpublished).
[51] D. Kielan and A. Marcinkowski, Z. Phys. A **352**, 137 (1995).
[52] S. K. Ghorai, P. M. Sylva, J. R. Williams, and W. L. Alford, Ann. Nucl. Energy **22**, 11 (1995).
[53] G. P. Vinitskaya, V. N. Levkovskiy, V. V. Sokol'skiy, and I. V. Kazachevskiy, Yad. Fiz. **5**, 1175 (1967).
[54] C. V. Srinivasa Rao, N. Lakshmana Das, B. V. Thirumala Rao, and J. Rama Rao, Curr. Sci. (Bangalore) **51**, 466 (1982).
[55] J. L. Casanova and M. L. Sanchez, An. Fis. Quim. **72**, 186 (1976).
[56] R. A. Sigg, Diss. Abstr. Int., B **37**, 2237 (1976).
[57] M. Valkonen, P. Homberg, R. Rieppo, J. K. Keinaenen and J. Kantele, University of Jyvaeskylae, Department of Physics, Report No. 1/1976, 1976 (unpublished).
[58] N. Ranakumar, E. Kondaiah, and R. W. Fink, Nucl. Phys. A **122**, 679 (1968).
[59] M. Bormann, E. Fretwurst, P. Schehka, G. Wrege, H. Buttner, A. Linder, and H. Meldner, Nucl. Phys. **63**, 438 (1965).
[60] V. N. Levkovskiy, Zh. Eksp. Teor. Fiz. **45**, 305 (1963).
[61] I. L. Preiss and R. W. Fink, Nucl. Phys. **15**, 326 (1960).
[62] S. Yasumi, J. Phys. Soc. Jpn. **12**, 443 (1957).
[63] J. L. Barreira Filho and H. U. Fanger, Ges. Kernen.-Verwertung, Schiffbau and Schiffahrt, Report No. 82, E, 1982, p. 8 (unpublished).
[64] V. K. Tikku, H. Singh, and B. Sethi, in *Proceedings of the Nuclear and Solid State Physics Symposium*, Chandigarh (1972), Vol. 2, p. 115.
[65] M. Bostan, E. Gueltekin, and I. A. Reyhancan, Ann. Nucl. Energy **30**, 1821 (2003).
[66] A. Marcinkowski, K. Stankiewicz, U. Garuska, and M. Herman, Z. Phys. A **323**, 91 (1986).

[67] S. Amemiya, K. Ishibashi, and T. Katoh, J. Nucl. Sci. Technol. **19**, 781 (1982).
[68] E. Gueltekin, V. Bostan, M. N. Erduran, M. Subasi, and M. Sirin, Ann. Nucl. Energy **28**, 53 (2001).
[69] C. V. Srinivasa Rao and J. Rama Rao, in *Proceedings of the International Conference on Nuclear Cross Sections for Technology*, Knoxville, TN, 1979 (National Bureau of Standards, USA, 1979), p. 848 .
[70] W. D. Lu, N. Ranakumar, and R. W. Fink, Phys. Rev. C **1**, 358 (1970).
[71] Y. Fujino, M. Hyakutake, and I. Kumabe, International Atomic Energy Agency, Report No. INDC(JAP)-51, 1977, p. 60 (unpublished).
[72] L. Chaturverdi, C. N. Pandey, and S. K. Bose, I.N.D.C. Secretariat, Report Series No. 61, 1977, p. 123 (unpublished).
[73] P. Cuzzocrea, E. Perillo, and S. Notarrigo, Nucl. Phys. A **103**, 616 (1967).
[74] S. Lulic, P. Strohal, B. Antolkovic, and G. Paic, Nucl. Phys. A **119**, 517 (1968).
[75] J. Brzosko, P. Decowski, K. Siwek-Diament, and Z. Wilhelmi, Nucl. Phys. **45**, 579 (1963).
[76] W. Struwe and G. Winkler, Nucl. Phys. A **222**, 605 (1974).
[77] G. P. Chursin, Ju. Gonchar, I. I. Zzaljubovskij, and A. P. Kljuchrev, Zh. Eksp. Teor. Fiz. **44**, 472 (1963).
[78] J. Brzosko, P. Decowski, K. Siwek-Diament and Z. Wilhelmi, Nucl. Phys. **74**, 438 (1965).
[79] E. Betak, R. Mikolajczak, J. Staniszewska, S. Mikolajewski, and E. Rurarz, Radiochim. Acta **93**, 311 (2005).
[80] S. S. Hasan, R. Prasad, and M. L. Seghal, Nucl. Phys. A **181**, 101 (1972).
[81] S. Murahira, Y. Satoh, N. Honda, A. Takahashi, T. Iida, M. Shibata, H. Yamamoto, and K. Kawade, International Atomic Energy Agency, Report No. INDC(JPN)-175, 1995, p. 171 (unpublished).
[82] D. C. Kceher, Nucl. Data Sheets **17**, 39 (1976).
[83] A. Hashizume and Y. Tendow, Nucl. Data Sheets **52**, 641 (1987).
[84] K. Kitao, Y. Tendow, and A. Hashizume, Nucl. Data Sheets **96**, 241 (2002).
[85] A. Poularikas, J. Cunningham, W. MC Millan, J. MC Millan, and R. W. Fink, J. Inorg. Nucl. Chem. **13**, 196 (1960).
[86] Fan Yangmei, Wang Zhihai, Han Rongdian, Wang Zhongmin, Liu Zhonglian, Du Huaijiang, and Xiao Zhenxi, Chin. J. Nucl. Phys. **10**, 108 (1988).
[87] J. Rama Rao, N. L. Singh, S. Singhal, A. V. Mohan Rao, S. Mukherjee, and L. Chaturvedi, Nucl. Instrum. Methods Phys. Res., Sect. B **17**, 368 (1986).
[88] N. I. Molla and S. M. Qaim, Nucl. Phys. A **283**, 269 (1977).
[89] N. I. Molla, S. M. Qaim, and H. Kalka, Phys. Rev. C **45**, 3002 (1992).
[90] R. Dóczi, V. Semkova, A. D. Majdeddin *et al.*, IAEA, Report No. INDC(HUN)-032, 1997 (unpublished).
[91] B. Lalremruata, S. Ganesan, V. N. Bhoraskar *et al.*, Ann. Nucl. Energy **36**, 458 (2009).
[92] S. Galanopoulos, R. Vlastou, C. T. Papadopoulos *et al.*, Nucl. Instrum. Methods Phys. Res., Sect. B **261**, 969 (2007).